Structural Engineering and Mechanics, Vol. 15, No. 2 (2003) 159-180
DOI: http://dx.doi.org/10.12989/sem.2003.15.2.159

Determination of crack spacing and crack width in reinforced concrete beams

R. Piyasena†, Yew-Chaye Loo‡ and Sam Fragomeni‡†

School of Engineering, Griffith University-Gold Coast Campus, Australia

(Received October 10, 2001, Revised August 10, 2002, Accepted December 5, 2002)

Abstract. In this paper spacing and width of flexural cracks in reinforced concrete beams are determined using two-dimensional finite element analysis. At early loading stages on the beam the primary crack spacing is based on the slip length, which is the development length required to resist the steel stress increment that occurs at a cracked section on the formation of the first flexural crack. A semi-empirical formula is presented in this paper for the determination of the slip length for a given beam. At higher load levels, the crack spacing is based on critical crack spacing, which is defined as the particular crack spacing that would produce a concrete tensile stress equal to the flexural strength of concrete. The resulting crack width is calculated as the relative difference in extensions of steel reinforcement and adjacent concrete evaluated at the cracked section. Finally a comparative study is undertaken, which indicates that the spacing and width of cracks calculated by this method agree well with values measured by other investigators.

Key words: analytical method; crack spacing; crack width; finite element analysis; reinforced concrete.

1. Introduction

Cracking in reinforced concrete is unavoidable due to its low tensile strength and extensibility. Wider cracks may not only destroy the aesthetics of the structure but also induce corrosion of steel reinforcement. Maximum allowable crack widths that will not induce corrosion for different environmental conditions have been specified by various authorities including ACI Committee 224 (1972). To ensure that the resulting crack widths under service loads do not exceed the limits set, designers may use the simple guidelines specified in relevant building codes. These guidelines are based on certain crack width prediction formulas proposed by various investigators. For example, guidelines for the distribution of tension steel specified by ACI Committee 318 (1995) are based on the following crack width prediction formula developed by Gergely and Lutz (1968), which is based on a statistical computer analysis of a large number of test results from different sources.

$$W_{t,\max} = 0.0132 f_s \sqrt[3]{cA_e} \times 10^{-3} \tag{1}$$

† PhD Student
‡ Professor and Head
‡† Senior Lecturer

In Eq. (1), $W_{t,\max}$ is the maximum crack width at the tension face of a member in mm, f_s is the steel stress at the cracked section in MPa, c is the concrete cover in mm measured to the centre of steel bars and A_e is the effective stretched concrete area in mm^2. Slightly different guidelines have been specified by Standards Australia International (2001). These guidelines nominate certain limits for the maximum steel stress, depending on the diameter and spacing of reinforcing bars. When the steel stresses under service loads do not exceed the above limits the resulting crack widths are deemed to be within the acceptable range.

In developing new prediction formulas, different researchers have used various procedures to calculate the spacing and width of cracks in reinforced concrete members. Watstein and Parsons (1943) and Chi and Kirstein (1958) developed empirical formulas to calculate the spacing and width of cracks in flexural members, based on experimental and analytical results of uniaxial tension members (cylindrical concrete prism with a central steel bar subjected to a tensile force). To determine the crack spacing, Broms (1965) calculated the concrete stresses by analysing a concrete section between two adjacent cracks, with the total bond force applied at the two ends of the block as uniformly distributed line loads at reinforcement level. Beeby (1970, 1971) used the analytical results of un-reinforced and reinforced concrete columns subjected to eccentric axial loads to evaluate the spacing and width of cracks. Bazant and Oh (1983) developed prediction formulas based on a theoretical study on the spacing and width of cracks, using the energy criterion of fracture mechanics as well as the strength criterion. To determine the spacing and width of cracks, Venkateswarlu and Gesund (1972) analysed a portion of a cracked beam between two adjacent cracks using two-dimensional finite element method, with the magnitude of the total bond force evaluated empirically using experimental results.

In this paper, a more rational approach is adapted in determining the spacing and width of cracks in reinforced concrete flexural members. Spacing and width of cracks are evaluated based on the concrete stress and strain distributions near flexural cracks, calculated using a rigorous analytical procedure. The bond force developed at the interface between reinforcement and surrounding concrete is evaluated by relating the bond stress to the local bond slip. The present method of calculation has wider applicability as it can include all the variables involved in reinforced concrete beams.

2. Analysis of concrete blocks adjacent to flexural cracks

To calculate crack spacing and crack width a series of analyses are carried out on various concrete block sections taken from loaded reinforced concrete beams. These concrete blocks are bounded by top and bottom faces of the beam and two transverse sections. The analyses are carried out by resorting to certain semi-empirical formulations in conjunction with the finite element method, with the details of the latter method described in Section 2.5. Two different types of concrete blocks are considered for this analysis. They are: (i) concrete block adjoining the first flexural crack in a beam, and (ii) concrete block located between two pair of adjacent flexural cracks. These two types are described below.

2.1 Concrete block adjoining the first flexural crack

Fig. 1(a) shows the concrete block analysed for the determination of concrete stresses and

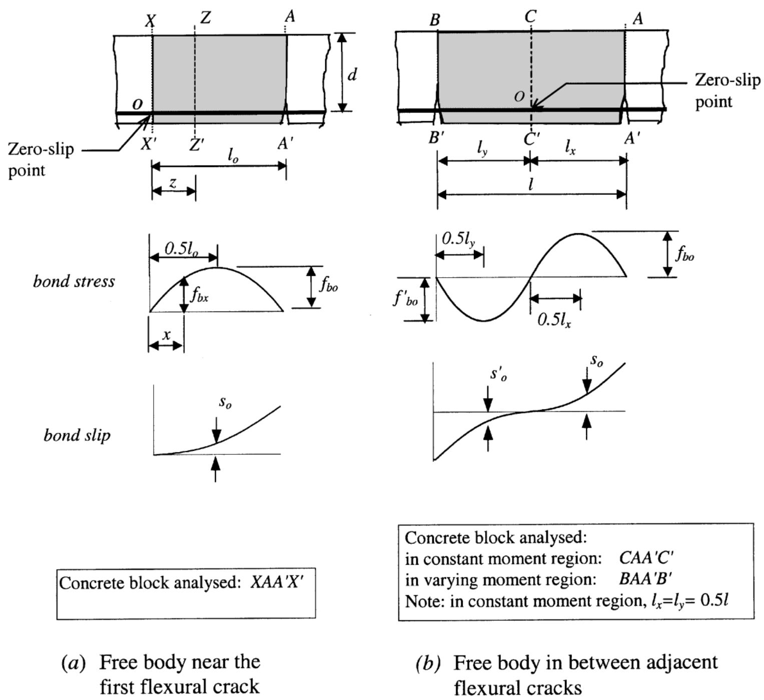

Fig. 1 Details of concrete blocks analysed

displacements adjacent to the first flexural crack in a beam. In this figure the transverse section *AA'*, bounding the concrete block, is taken through the first flexural crack in the beam. The formation of this crack increases the tensile force in steel bars at section *AA'*, as the concrete tensile force is transferred to the reinforcement. This force increment is resisted by bond forces developed along a particular length (development length) of steel bars on either side of the crack. The end point of this development length on one side of the crack (section *XX'* in Fig. 1a) is taken as the other boundary of the concrete block analysed. This length, shown as l_o in Fig. 1(a), is herein referred to as the slip length, where stresses at sections beyond a distance l_o away from the crack are unaffected by the formation of the first crack. The magnitude of the slip length l_o and the associated bond force for a given beam are determined using the procedure described in Section 2.3.1.

Compressive and tensile forces acting on the two end transverse sections (*AA'* and *XX'*) are calculated assuming a linear strain distribution across the depth of the beam, and satisfying translational and rotational equilibrium requirements. For the translational equilibrium, total compressive force acting on the section is equated to the total tensile force, including the effect of reinforcement. For the rotational equilibrium, moment due to all compressive and tensile forces about the neutral axis is made equal to the applied bending moment at the section. In this calculation, the applied bending moment at the cracked section (*AA'*) is taken as the cracking moment of the beam, M_{cr}. In a constant moment region, the moment at the uncracked section *XX'* is also equal to M_{cr}, while in a varying moment region its value depends on the loading regime on the beam. Note that in the process of calculating the concrete stresses, the resulting steel stresses f_{s1} and f_{s2} at *XX'* and *AA'* respectively, are also determined. These steel stresses are used in the evaluation of bond forces developed between reinforcement and surrounding concrete (Section 2.3.1).

2.2 Concrete block in between two adjacent cracks

The concrete block shown in Fig. 1(b) is analysed to determine the concrete stresses and displacements in between two adjacent cracks in a loaded beam. This analysis is carried out for different values of crack spacing and load levels (represented by various steel stress values at cracked sections) to investigate their effect on the resulting maximum tensile stress within the concrete block.

In a constant moment region, the concrete block *BAA'B'* is symmetrical about the centre line *CC'* (Fig. 1b), and therefore only one half of the block (*CAA'C'*) is analysed. For a selected value of steel stress at cracked section *AA'*, the resulting concrete compressive force is determined by assuming a linear strain distribution across the depth of the beam, and equating the concrete compressive force and steel tensile force at the section.

In a varying moment region, the full block *BAA'B'* is analysed. The steel stress at the cracked section *AA'* is selected to represent the loading regime on the beam. The resulting concrete compressive force at this section is determined using the same procedure described in the previous paragraph.

The concrete compressive force and steel stress at the other cracked section *BB'* are determined by assuming a linear strain distribution across the depth of the beam and satisfying the translational and rotational equilibrium of the section. This procedure is same as that described in Section 2.1 for calculating forces at the cracked section *AA'* in the concrete block adjoining the first flexural crack (see Fig. 1a). For this calculation, the bending moment at section *BB'* is evaluated using the selected steel stress at section *AA'* and the loading on the beam. The evaluation of bond forces is described in the following Section.

2.3 Bond forces acting on concrete blocks

To evaluate bond forces, the bond stress is assumed to vary parabolically along the steel bar as shown in Fig. 1. This assumption is followed by the test results of Mains (1951) and Jian *et al*. (1984), which showed a similar pattern. The magnitude of the peak bond stress at the mid point of the parabolic distribution is determined by relating its value to the slip at that point, and satisfying the equilibrium of forces acting on the steel bar. This procedure is described below.

2.3.1 Bond stress near the first flexural crack and the slip length l_o

By equating the total bond force acting on the bar surface and the difference in tensile forces at the two ends of a reinforcing bar between sections *AA'* and *XX'* (see Fig. 1a), the following equation is derived.

$$\frac{\pi\phi^2}{4}(f_{s2} - f_{s1}) = \frac{2}{3}\pi\phi f_{bo} l_o \qquad (2)$$

where f_{s2} and f_{s1} are the stresses in the steel bar at the cracked section *AA'* and the uncracked section *XX'*, respectively and ϕ is the bar diameter. Values of f_{s1} and f_{s2} are calculated as previously described in Section 2.1, while f_{bo} is the peak bond stress and l_o is the slip length, both unknown.

Also the peak bond stress f_{bo} at the mid point of the parabolic distribution can be related to the slip s_o occurring at that point. The slip is calculated as the relative difference in extensions of steel and surrounding concrete. The steel extension is calculated by integrating the strain function, as the steel stress between sections *AA'* and *XX'* varies non-linearly due to the parabolic bond stress distribution. This procedure is described below.

Using the parabolic distribution, the bond stress f_{bx} at a distance x from the zero-slip section (see Fig. 1a) can be expressed as

$$f_{bx} = 4f_{bo}\frac{x}{l_o}\left(1-\frac{x}{l_o}\right) \qquad (x \le l_o) \tag{3a}$$

The total bond force F_{bz} acting on the bar surface between sections *XX'* and *ZZ'* (Fig. 1a) can then be calculated using the following integral.

$$F_{bz} = \int_{x=o}^{x=z} \pi\phi f_{bx}dx = \frac{4f_{bo}\pi\phi}{l_o}\left(\frac{z^2}{2}-\frac{z^3}{3l_o}\right) \qquad (z \le l_o) \tag{3b}$$

where z is the distance to the section *ZZ'* from the zero-slip section (Fig. 1a).

The resulting steel stress f_{sz} at the section *ZZ'* can be calculated using the following equation, which is derived by equating the difference in tensile forces acting at sections *XX'* and *ZZ'* of the steel bar, and the total bond force on the bar surface between those two sections.

$$\frac{\pi\phi^2}{4}(f_{sz}-f_{s1}) = F_{bz} \tag{3c}$$

Substitution of Eq. (3c) into Eq. (3b) leads to the following equation for f_{sz}.

$$f_{sz} = f_{s1} + \frac{16f_{bo}}{l_o\phi}\left(\frac{z^2}{2}-\frac{z^3}{3l_o}\right) \qquad (z \le l_o) \tag{3d}$$

The corresponding steel strain ε_{sz} at the section *ZZ'* is then calculated as $\varepsilon_{sz} = f_{sz}/E_s$ where E_s is the elastic modulus of steel. The resulting extension of the steel bar, e_{so}, at the mid point of the parabolic bond stress distribution is calculated by integrating the steel strain function ε_{sz} as follows.

$$e_{so} = \int_{z=o}^{z=0.5l_o}\varepsilon_{sz}dz = \int_{z=o}^{z=0.5l_o}\left\{\frac{f_{s1}}{E_s} + \frac{16f_{bo}}{l_o\phi E_s}\left(\frac{z^2}{2}-\frac{z^3}{3l_o}\right)\right\}dz = \frac{f_{s1}l_o}{2E_s} + \frac{f_{bo}l_o^2}{4E_s\phi} \tag{3e}$$

In calculating e_{so}, the use of f_{s2} (steel stress at the cracked section) is considered more appropriate than the use of f_{s1} (steel stress at the zero-slip section), because the crack spacing and crack width are usually expressed as a function of f_{s2}. Therefore, the variable f_{s1} in Eq. (3e) is changed to f_{s2} using the following relationship, which is derived by re-arranging Eq. (2).

$$f_{s1} = f_{s2} - \frac{8f_{bo}l_o}{3\phi} \tag{3f}$$

Substitution of Eq. (3f) into Eq. (3e) yields the following formula for the calculation of e_{so}.

$$e_{so} = \frac{f_{s2}l_o}{2E_s} - \frac{13f_{bo}l_o^2}{12E_s\phi} \tag{3g}$$

where the elastic modulus of steel is taken as E_s = 200000 MPa.

Then the slip s_o at the mid point between sections *XX'* and *AA'* is calculated as

$$s_o = e_{so} - e_{co} \tag{4}$$

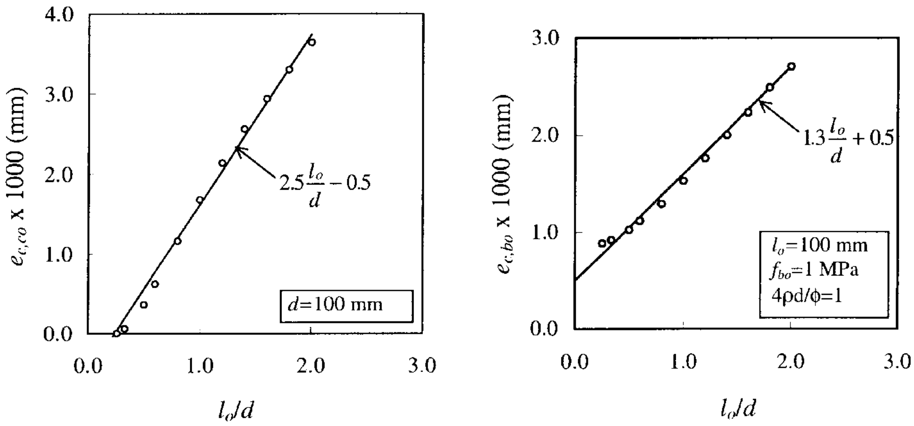

(*a*) extension due to compressive force at cracked section

(*b*) extension due to bond force

Fig. 2 Approximation for concrete extensions

where e_{co} is the extension of concrete at the mid point between sections *AA*' and *XX'* which is calculated as

$$e_{co} = e_{c,\,co} + e_{c,\,bo} \tag{5}$$

in which $e_{c,\,co}$ is part of the extension due to the concrete compressive force acting at the cracked section, and $e_{c,\,bo}$ is that part due to the bond force.

Calculation of $e_{c,\,co}$ and $e_{c,\,bo}$

Values of $e_{c,\,co}$ and $e_{c,\,bo}$ were calculated for a large number of beam sections similar to *XAA'X'* shown in Fig. 1(a), using the finite element method which is described later in Section 2.5. The results showed that $e_{c,\,co}$ is proportional to the effective depth d, if the ratio l_o/d remains unchanged. Therefore, for convenience, $e_{c,\,co}$ is calculated using a value of d = 100 mm, and the results are multiplied by the ratio $d/100$ (d is in mm) to obtain the final extension. The results also showed that $e_{c,\,co}$ varies almost linearly with l_o/d as shown in Fig. 2(a). Consequently, $e_{c,\,co}$ (in mm) can be expressed as a function of $d/100$ and l_o/d as follows.

$$1000 e_{c,\,co} = \left(2.5\frac{l_o}{d} - 0.5\right)\frac{d}{100} \geq 0 \tag{6a}$$

The calculated values of the concrete extension due to bond forces $e_{c,\,bo}$ showed that if the ratio l_o/d remains unchanged, $e_{c,\,bo}$ is proportional to f_{bo}, l_o, and the total perimeter of steel bars per unit width of the beam, which is equal to $4\rho d/\phi$. Therefore, for convenience, $e_{c,\,bo}$ is calculated using f_{bo} = 1 MPa, $4\rho d/\phi$ = 1 and l_o = 100 mm, and the results are multiplied by the actual values of f_{bo}, $4\rho d/\phi$ and the ratio $l_o/100$ (l_o is in mm) to obtain the final extension. Further, the results showed that $e_{c,\,bo}$ varies almost linearly with l_o/d as shown in Fig. 2(b). Therefore, $e_{c,\,bo}$ (in mm) can be expressed in terms of f_{bo}, $4\rho d/\phi$, $l_o/100$ and l_o/d as follows.

$$1000 e_{c,\,bo} = \left(1.3\frac{l_o}{d} + 0.5\right)\left(\frac{l_o}{100}\right)\left(\frac{4\rho d}{\phi}\right) f_{bo} \geq 0 \tag{6b}$$

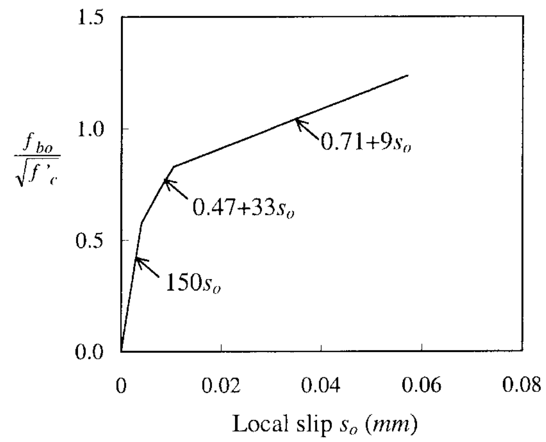

Fig. 3 Bond stress-bond slip relationship used (proposed by Giuriani *et al.* 1991, for deformed bars with stirrups)

In determining the two unknowns f_{bo} and l_o using Eqs. (2) to (6), the bond stress-bond slip relationship shown in Fig. 3 is utilised to relate s_o and f_{bo}. This relationship has been developed by Guiriani *et al.* (1991) using the results of pull out tests on deformed bars with transverse reinforcement (stirrups), carried out by Eligehausen (1983). As this relationship is non-linear, the above equations are solved by a trial and error procedure.

It must be noted that the bond stress obtained using Fig. 3 needs to be modified before substituting into Eqs. (2) to (6) because, for the same slip value, different bond stresses may develop at various points along the steel bar depending on the distance from the crack. This fact was revealed by the experimental results of Nilson (1972). These results have shown that, for a particular slip value, the bond stress developed at different points along a steel bar increases almost linearly with the distance from the crack, up to a distance of 100 mm. At points where the distance from the crack is in between 100 and 153 mm, only a small difference was observed in bond stresses developed for a particular slip value, while no difference was noted in bond stresses developed at points that are more than 153 mm away from the crack.

The limiting distance of 100 mm mentioned in the previous paragraph was observed in experiment results (Nilson 1972) involving a single bar size with diameter 25.4 mm. It is assumed that this limiting distance depends on the bar diameter when different bar sizes are used. To be consistent with experimental results of Nilson (1972) this limiting distance is taken as 4ϕ where ϕ is the bar diameter. Consequently, if the peak bond stress occurs at a distance more than 4ϕ away from the crack ($0.5l_o > 4\phi$), the value of f_{bo} obtained from Fig. 3 is used in the calculation with no modification. If the peak bond stress occurs at a closer distance, the bond stress obtained from Fig. 3 is reduced proportionately depending on the distance from the crack. To facilitate this reduction, the peak bond stress f_{bo} obtained from Fig. 3 is multiplied by a factor γ, which is taken as unity if the peak bond stress occurs at a distance larger than 4ϕ from the crack, and reduced proportionately for smaller distances using the following equation.

$$\gamma = \frac{0.5l_o}{4\phi} \leq 1 \tag{7}$$

where $0.5l_o$ is the distance from the crack to the point where the peak bond stress f_{bo} occurs (Fig. 1a). Hence the relationship between the peak bond stress f_{bo} and the slip s_o can be expressed in general form as

$$f_{bo} = \gamma\Gamma(s_o) \tag{8}$$

where $\Gamma(s_o)$ is the bond stress corresponding to the slip s_o obtained from the relationship shown in Fig. 3.

2.3.2 Bond stress in between adjacent flexural cracks

Bond forces acting on concrete blocks located between adjacent flexural cracks are calculated by solving the equations presented in the previous Section (Eqs. (2) to (8)), with the variable l_o changed as appropriate. In this calculation the trial and error procedure described in Section 2.3.1 is slightly modified depending on whether the concrete block is located in a constant or varying moment region, as described below.

(a) Constant moment region

It can be seen that the half-concrete block analysed in a constant moment region (*CAA'C'* in Fig. 1) is similar to the block adjacent to the first flexural crack (*XAA'X'*) in every respect, except that their lengths are different. In calculating the bond force in block *CAA'C'*, the variable l_o in Eqs. (2) to (8) is therefore replaced by $0.5l$ where l is the selected value of the crack spacing (see Fig. 1). The two unknowns determined by solving these equations are the peak bond stress f_{bo} and the steel stress f_{s1} at mid section *CC'*, in contrast to f_{bo} and l_o evaluated for the block *XAA'X'*.

(b) Varying moment region

In determining the peak bond stresses in the concrete block *BAA'B'* (see Fig. 1), a trail value is first assumed for the distance l_x, and the procedure described in the previous paragraph is used for the two blocks *BCC'B'* and *CAA'C'* separately to calculate f'_{bo} and f_{bo}. This will generally yield two different f_{s1} values (steel stress at mid section *CC'*) for the two blocks. The trial distance l_x is changed and the calculation is repeated until the difference in the two f_{s1} values becomes negligible, when the values of l_x, f_{bo}, f'_{bo} and f_{s1} are taken as final.

2.4 Calculation of maximum crack width at reinforcement level

Only crack widths in constant moment regions are calculated because, at the same load level, the crack widths in varying moment regions are smaller, as described later in Section 4.2.2.

The width of a crack at reinforcement level is determined as the relative difference in extensions of steel bars and adjacent concrete. The extension of steel bars e_{s1} for the length $0.5l$ from section *CC'* to *AA'* in Fig. 1(b) is calculated using the following equation.

$$e_{s1} = \frac{f_{s2}l}{2E_s} - \frac{f_{bo}l^2}{3E_s\phi} \tag{9}$$

where l is the crack spacing and f_{s2} is the steel stress at the cracked section *AA'*. Eq. (9) has been derived using the procedure described for evaluating e_{so} (Eq. (3a) to (3g)) with the following changes: (i) in Eq. (3a), replace l_o with $0.5l$ (see Fig. 1), and (ii) in Eq. (3e), change the upper limit of integration from $z = 0.5l_o$ to $z = 0.5l$.

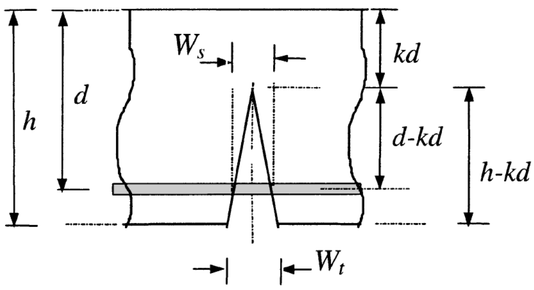

Fig. 4 Relationship between crack widths at reinforcement level and at tension face

The resulting crack width W_{s1} is then calculated as

$$W_{s1} = e_{s1} - e_{c1} \tag{10}$$

where e_{c1} is the extension of concrete adjacent to steel bars. Its value is taken as twice the corresponding extension at the mid section between *CC'* and *AA'* in Fig. 1(b). ($e_{c1} = 2e_{co}$ where e_{co} is calculated using Eqs. (5) and (6) with l_o replaced by $0.5l$).

Note that in calculating the maximum crack width, both crack spacings on either side of section *AA'* are assumed to be equal to the maximum crack spacing $l_{\max}$. This is because the crack width is found to increase with the spacing of adjacent cracks as described later in Section 3.2.2. Determination of $l_{\max}$ is described in Section 4.2.1. Thus the total crack width W_s at the reinforcement level can be calculated as

$$W_s = 2W_{s1.} \tag{11}$$

The resulting crack width W_t at the tension face of the beam is evaluated by assuming the two faces of the crack to be planar (Fig. 4). Then the crack width at the tension face W_t can be calculated as a proportion of W_s using the following formula.

$$W_t = \left(\frac{h - kd}{d - kd}\right)W_s \tag{12}$$

where *kd* is the depth of the compression zone and *h* is the overall height of the beam (Fig. 4).

In the present method of calculating concrete stresses and extensions in loaded beams, it is assumed that the loading is incremented in small steps. At a selected load level, equilibrium conditions and the bond stress - bond slip relationship are applied to concrete sections as described above, only after the flexural cracks corresponding to that load level have fully grown, the bond slip taken place, and the full bond stress has developed. At this stage, concrete blocks between successive cracks have reached a state of static equilibrium. Hence, after the flexural cracks in the beam have stabilised, linear elastic analysis can be performed on concrete blocks between adjacent cracks to determine the stresses and extensions. This analysis is carried out using two-dimensional linear elastic finite element method as described below.

2.5 Finite element analysis

Fig. 5 shows a unit width of a typical concrete block isolated for the analysis. This block is divided into 240 rectangular elements by 24 longitudinal and 10 transverse divisions. The

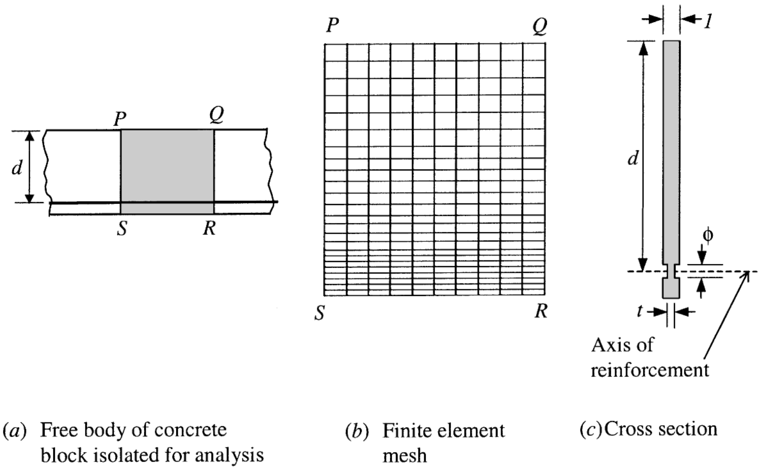

Fig. 5 Finite element mesh and cross section for rectangular beams

longitudinal divisions near the axis of reinforcement are taken at closer intervals to have a finer mesh (Fig. 5). As shown in Fig. 5, the width of the block at reinforcement level is reduced to account for the reduction in concrete area due to steel bars. The reduced thickness t at the reinforcement level, corresponding to a unit width of the beam is calculated using the following formula.

$$t = 1 - \frac{\rho d}{\phi} \tag{13}$$

The analysis is carried out using the standard software package STRAND6 (1993). A four-node rectangular plane stress element is used in the analysis. This element is generated by the software by assembling four Constant Strain Triangular (CST) elements with the internal fifth node condensed out. The CST element used by STRAND6 (1993) has been developed using the theory described by Zienkiewicz (1977) and Cook *et al.* (1989).

3. Results

A large number of concrete blocks isolated from various loaded beams comprising of rectangular, T-shaped as well as Box-shaped cross sections were analysed using the procedure described in Section 2. The results obtained from this analysis are summarised below.

3.1 Concrete blocks adjoining the first flexural crack

3.1.1 Slip length l_o

Slip length l_o is calculated by solving Eqs. (2) to (8) for different beams having various material and sectional properties. Table 1 shows the parameters and their ranges used. Bar diameters ranging from 10 mm to 32 mm were used to achieve the different reinforcement ratios listed in Table 1. Table 2 gives certain constraints applied on reinforcement ratio and bar diameter to ensure that each

Table 1 Parameters and their ranges used to calculate l_o

Parameter	Range	Number of values
Concrete strength, f_c'	20-50 MPa	4
Reinforcement ratio, ρ	0.003-0.030	5
Flange width/web width, b/b_w	1.0-3.0	5
Flange thickness/effective depth, h_f/d	0.25-0.40	4
Effective depth, d	100-600 mm	6

Table 2 Ranges of reinforcement ratio and bar diameter used to calculate l_o

Effective depth, d (mm)	Member width, b (mm)	Reinforcement ratio, ρ		Bar diameter, ϕ (mm)	
		Lower limit	Upper limit	Lower limit	Upper limit
100	1000	0.0035	0.075	10	12
200	1000	0.005	0.01	12	20
300	200	0.01	0.02	16	22
400	240	0.01	0.025	20	25
500	300	0.01	0.025	25	28
600	400	0.01	0.03	28	32

beam represents a common practical situation. Note that only rectangular sections were considered for members with effective depths 100 mm and 200 mm. For beams with effective depths ranging from 300 mm to 600 mm, both T-shaped and box-shaped sections were considered, in addition to rectangular sections. Various combinations of the parameters listed in Table 1, subjected to the above constraints, have produced 3240 different beams. For all the beams the ratio of effective depth to the overall height (d/h) is taken as 0.87. It can be seen that the prediction formulas developed in this Section are also applicable for other values of d/h ratios, as demonstrated by comparison of results (Section 5).

For each beam described above, the steel stress increment that occurs at the first flexural crack Δf_{so} is also determined using Eq. (2), after calculating the slip length l_o and the peak bond stress f_{bo}. Note that $\Delta f_{so} = f_{s2} - f_{s1}$ where f_{s1} and f_{s2} are the steel stresses at the uncracked section *XX'* and the cracked section *AA'* respectively (Fig. 1a), both calculated for the same bending moment $M = M_{cr}$. The calculated values of l_o and Δf_{so} for the above 3240 beams showed that l_o increases with Δf_{so} and bar diameter ϕ, while it decreases with the concrete strength f_c'. Consequently, using the above calculated values in a semi-regression analysis, the following empirical formula was developed to determine the slip length in terms of f_c', ϕ and Δf_{so}.

$$l_o = 100 + \left(1.3 - \frac{f_c'}{80}\right)\left(0.25 + \frac{\phi}{28}\right)\Delta f_{so} \tag{14}$$

where Δf_{so} and f_c' are in MPa, and l_o and ϕ are in mm.

The results also showed that Δf_{so} decreases with the reinforcement ratio, while it increases with concrete strength. Using the calculated values in a semi-regression analysis, the following formula was developed to determine the steel stress increment Δf_{so} at the first flexural cack in reinforced concrete members.

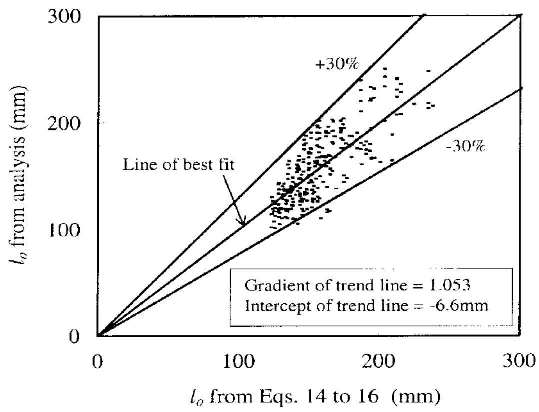

Fig. 6 Comparison of l_o computed using empirical formulas and 'exact' values

$$\Delta f_{so} = \frac{(0.3 + 0.0125 f_c')}{\rho_x} \tag{15}$$

in which $\rho_x = \rho$, for rectangular sections, (16a)

and, $\rho_x = \rho\left(1.4 - 0.4\frac{b}{b_w}\right)\frac{b}{b_w}$, for T- and Box-sections, (16b)

In Eq. (16), b is the flange width and b_w is the web width. Note that for box sections, the flange width is the total width of the member, while the web width is twice the wall thickness.

A comparison of the slip lengths calculated using the proposed empirical formulas (Eqs. (14) to (16)) and the 'exact' values determined by solving Eqs. (2) to (8) is shown in Fig. 6, for 300 typical beams. Ranges of variables included in this calculation are as follows: f_c' = 20 – 50 MPa, ρ = 0.0035 – 0.03, b/b_w = 1.0 – 2.5, and ϕ = 10 – 30 mm. It may be seen that more than 98 percent of the 'exact' l_o values (except the five values lying below the negative 30% line) fall between ±30% of those calculated using the empirical formulas. It will be shown in Section 4.1 that, in a beam subjected to a gradually increasing load, the spacing of primary cracks can be related to the slip length l_o. This prediction will be verified in Section 5.

3.1.2 Concrete stress at the tension face

The concrete block adjacent to the first flexural crack (block *XAA'X'* in Fig. 1a) in six different beams were analysed by the finite element method to investigate the concrete stress distribution at the tension face. Table 3 shows the details of these beams. Values of l_o and Δf_{so}, calculated using Eqs. (14) to (16) are also shown in the same Table. Note that the concrete strength for all these beams was taken to be constant, f_c' = 32 MPa, as the concrete stress distribution was found to be insensitive to f_c'. Each of the above beams was analysed twice, firstly for a constant moment region, and next for a varying moment region that corresponds to a beam under a central point load (total 12 cases).

Results of the above analyses indicate that the concrete stress at the tension face near the first flexural crack increases gradually from zero at the crack to a maximum value at the end of the slip length. Although the maximum value of this concrete tensile stress and the slip length vary from one beam to another, the gradual variation of the concrete tensile stress along the slip length is

Table 3 Details of beams used to calculate concrete stress and crack width

Beam No.	Width (mm)	Effective depth (mm)	Total height (mm)	Reinforcements	Reinforcement Ratio	l_o (mm)	Δf_{so} (MPa)
B1	1000	170	200	12ϕ @ 165 mm	0.004	207	175
B2	1000	170	200	16ϕ @ 145 mm	0.008	165	88
B3	1000	170	200	12ϕ @ 110 mm	0.006	171	117
B4	200	400	450	$3 \times 16\phi$	0.0075	169	93
B5	315	400	450	$4 \times 20\phi$	0.010	161	70
B6	325	400	450	$4 \times 25\phi$	0.015	148	47

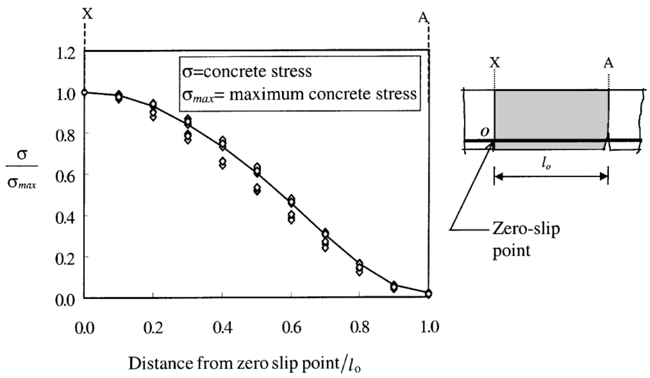

Fig. 7 Variation of concrete stress at the tension face near the first flexural crack

found to have a similar pattern for all the 12 beams analysed. A typical variation is shown in Fig. 7. This gradual variation of the concrete tensile stress along the slip length will be utilised later in Section 4 to predict the locations of subsequent flexural cracks that are formed at early loading stages of a beam.

3.2 Concrete blocks in between cracks

3.2.1 Concrete stress distribution between adjacent cracks

To investigate the stress distribution in between two adjacent cracks, concrete blocks *BAA'B'* and *CAA'C'* shown in Fig. 1(b) were analysed for the same six beams detailed in Table 3. The analysis was carried out for different crack spacings (l values) at various load levels (f_{s2} values) shown in Table 4, for concrete blocks located in a constant moment region and a varying moment region that corresponds to a beam under a central point load (total 72 cases).

Results show that the maximum concrete tensile stress across any transverse section between two adjacent cracks occurs at the level of reinforcement. It is also seen that the magnitude of this maximum concrete tensile stress varies along the reinforcing bar between the two cracks. In constant moment regions, the peak value of the maximum concrete tensile stress at reinforcement level occurs at the mid point between the two cracks. In varying moment regions, the location of this peak value is found to depend on the magnitudes of bending moments at the two adjacent cracked sections.

Table 4 Values of f_{s2} and l used to calculate concrete stress and cack width

B1		B2		B3		B4		B5		B6	
f_{s2} (MPa)	l (mm)	f_{s2} (MPa)	l (mm)	f_{s2} (MPa)	l (mm)	f_{s2} (MPa)	l (mm)	f_{s2} (MPa)	l (mm)	f_{s2} (MPa)	l (mm)
	200		160		180		200		160		150
220	250	150	200	200	200	150	250	150	200	150	180
	300		300		250		300		250		210
220		100		200		130		130		80	
250	300	150	200	250	250	160	200	160	200	120	200
300		200		300		200		200		160	

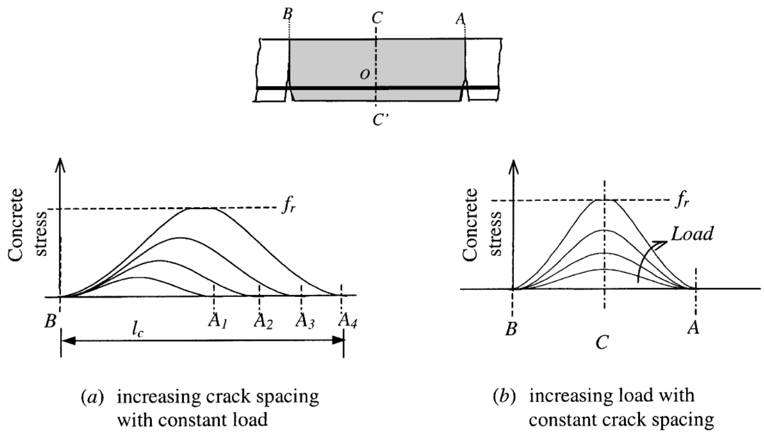

Fig. 8 Variation of concrete tensile stresses at reinforcement level in between adjacent cracks (f_r = flexural strength of concrete)

Critical crack spacing l_c

The results show that the peak value of the maximum concrete tensile stress at reinforcement level increases with the loading on the beam, as well as the spacing between adjacent cracks (see Fig. 8). The particular crack spacing which produces a tensile stress equal to the flexural strength of concrete (BA_4 in Fig. 8a) is herein referred to as the critical crack spacing, l_c for the given load level. The calculated values of critical crack spacing for the 72 cases investigated indicate that l_c decreases gradually with the increase of the loading on the beam.

3.2.2 Crack width

The crack width at the tension face W_t was calculated using the procedure described in Section 2.4 for the same 72 beam sections mentioned previously (See Tables 3 and 4). The results show that the crack width increases with the loading on the beam as well as the spacing of adjacent cracks.

It can be seen in Eq. (12) that the relationship between W_s and W_t depends on the depth of the compression zone kd at the cracked section (See Fig. 4). Crack width results of the above 72 beams show that this relationship is not significantly affected by different k values encountered in the calculation. It is also seen that accurate results can be obtained for W_t by assuming a constant value

k = 0.3, which corresponds to moderately reinforced beams. Using this assumption, Eq. (12) can be simplified as

$$W_t = W_s\{1.43(h/d) - 0.43\}. \tag{17}$$

4. Propagation of flexural cracks

Flexural cracks are categorised into two groups namely, (i) primary cracks, and (ii) secondary cracks. Primary cracks are defined as the cracks that are developed after the maximum bending moment at any section within the beam has exceeded the cracking moment. Secondary cracks are those cracks formed in between existing cracks at higher load levels, after the formation of primary cracks is completed.

4.1 Primary crack spacing

The location of primary cracks is predicted using the slip length l_o and the distribution of concrete stress at the tension face near the first flexural crack already discussed in Section 3.1. Spacing of these cracks for constant and varying moment regions are different, as described in the following Sections.

4.1.1 Constant moment region

Fig. 9 shows a simply supported beam subjected to two equal point loads equally spaced from the mid span, so that the bending moment within the middle region is constant. The line *ACDB* indicates the resulting concrete stress f_R at the tension face of the beam, which has the same shape as the bending moment diagram. The line *A'B'* represents the flexural strength f_r at the tension face, which may vary slightly from one section to another.

When the load on the beam is increased from zero, the first flexural crack occurs at a section such as X_1, which has the lowest flexural strength within the constant moment region. Once this crack is formed, the concrete stress at the tension face will become zero at the crack, and gradually increases along the slip length l_o, as already described in Section 3.1. The modified stress pattern on the tension face is schematically shown by curved lines in Fig. 9. As a result of this modification, new cracks can only develop at sections more than a distance l_o away from the first crack at X_1. This is because the concrete tensile stress within a distance l_o from the crack is much lower than the rest. This

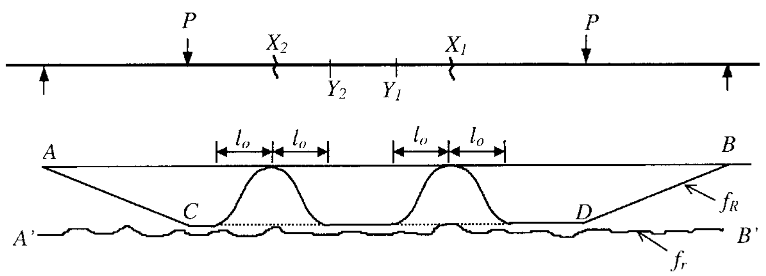

Fig. 9 Propagation of primary cracks in a constant moment region

means that the primary crack spacing l_p in a constant moment region should be larger than l_o $(l_p \geq l_o)$.

If the load is increased slightly, a second crack will develop at a section such as X_2 (Fig. 9) that has the next lowest flexural strength within the constant moment region, and more than a distance l_o away from the first crack. Formation of this crack will also modify the concrete stress at the tension face of the beam for a distance l_o on either side of the new crack at X_2, as shown in Fig. 9. It is clear in this figure that a slight increase in the load may develop another new crack in between the sections at Y_1 and Y_2, if the distance X_1X_2 is larger than $2l_o$. This means that the primary crack spacing in a constant moment region will not exceed $2l_o$ $(l_p \leq 2l_o)$. Therefore, the primary crack spacing l_p in a constant moment region should satisfy the following equation.

$$l_o \leq l_p \leq 2l_o \tag{18}$$

where l_o is the slip length.

4.1.2 Varying moment region

To predict the formation of primary cracks in a varying moment region, a simply supported beam subjected to a central point load shown in Fig. 10 is considered. The line *ACB* indicates the concrete stress at the tension face of the beam before any cracks are formed, while the line *A'B'* represents the flexural strength. It is clear that the first flexural crack is formed at the mid-span of the beam (point X_1) where the concrete stress at the tension face is largest.

Once the first crack is formed at X_1, the concrete stress at the tension face will modify for a distance l_o on either side of the crack as shown by the curved lines. It can be seen that the concrete tensile stresses at sections X_2 and X_2' will next reach the flexural strength of concrete, if the load is increased further. This means that two new cracks will develop at sections that are a distance l_o away on either side of the first crack. Formation of these cracks will also modify the concrete stress at the tension face, as shown by the curved lines. As a result of this modification, under an increasing load on the beam, two more new cracks will develop at X_3 and X_3' which are l_o away from cracks at X_2 and X_2', respectively. This suggests that all primary cracks in a varying moment region are formed at a regular spacing of l_o. Therefore in a varying moment region the primary crack spacing can be expressed as

$$l_p = l_o. \tag{19}$$

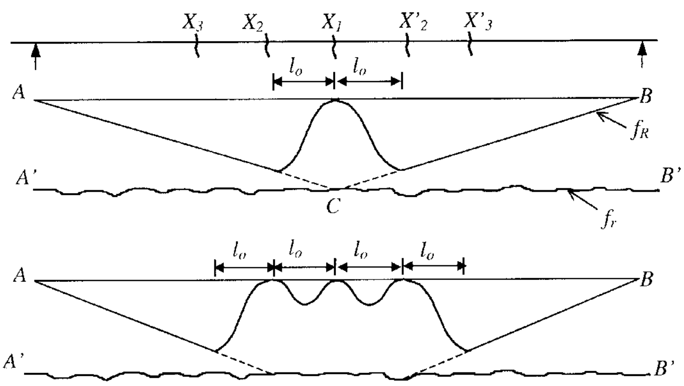

Fig. 10 Propagation of primary cracks in varying moment regions

4.2 Secondary crack spacing

Spacing of secondary cracks under a given load level is predicted in the following Sections, using the critical crack spacing l_c. Spacing of these cracks are different for constant and varying moment regions as described below.

4.2.1 Constant moment region

As seen in Fig. 8(a), for crack spacings larger than the critical crack spacing l_c, the maximum concrete tensile stress at reinforcement level exceeds the flexural strength of concrete, which causes a new crack to form. This means that the maximum crack spacing $l_{\max}$ at a given load level should be equal to the critical crack spacing l_c ($l_{\max} = l_c$).

Similarly, if the crack spacing is equal to the critical crack spacing l_c, any increase in the load on the beam will cause the maximum concrete tensile stress at reinforcement level to exceed the flexural strength of concrete (see Fig. 8b). This will result in the formation of a new crack at the mid section *CC'*, dividing the crack spacing l_c into two halves. This means that the minimum crack spacing at this load level is $0.5l_c$, because crack spacings previously divided into two halves at lower load levels are larger than l_c. This follows from the fact that critical crack spacing l_c decreases with the increased load on the beam. Therefore, the minimum crack spacing $l_{\min}$ at this load level should be equal to $0.5l_c$ ($l_{\min} = 0.5l_c$).

As described in the previous two paragraphs, at a given load level, the individual crack spacings in a constant moment region will lie between the upper limit l_c and the lower limit $0.5l_c$. As a result, the measured average crack spacing l_{ave} at this load level may vary between these two limits. i.e.,

$$0.5 l_c \leq l_{ave} \leq l_c \, . \tag{20}$$

The predicted average crack spacing $l_{ave\text{-}pred}$ at this load level can be taken as the arithmetic mean of these two limits as

$$l_{ave\text{-}pred} = 0.75 l_c . \tag{21}$$

4.2.2 Varying moment region

As described in Section 4.1.2, primary crack spacing in a varying moment region is small, and is equal to l_o (Eq. 19). This is in contrast to a constant moment region where larger crack spacings are present because the primary crack spacing varies between l_o to $2l_o$ (Eq. 18). Results of the finite element analyses indicate that, if the crack spacing is small and equal to l_o, the concrete tensile stress within the block will not reach the flexural strength, even when the load is close to the ultimate load. (Note that the maximum concrete tensile stress is low for smaller crack spacings as shown in Fig. 8a.) As a result, in a varying moment region the formation of secondary cracks is very rare, and the average crack spacing remains constant during the whole loading period. Therefore the predicted average secondary crack spacing in a varying moment region, at all load levels, can be expressed as

$$l_{ave\text{-}pred} = l_o . \tag{22}$$

It may be noted that smaller crack spacings in varying moment regions result in smaller crack widths when compared with constant moment regions at the same load level. This is because the crack width increases with the spacing of adjacent cracks as previously described in Section 3.2.2.

5. Comparison of predicted and measured values

5.1 Primary crack spacing

To verify the accuracy of proposed prediction formulas, the primary crack spacings calculated by Eqs. (18) and (19) are compared with the values measured by other investigators. Although many investigations have been carried out on cracking of reinforced concrete beams, results of individual crack spacing are rarely available; only the average crack spacing is reported most of the times. Stewart (1997) has reported the results of individual crack spacing on two simply supported and two continuous box-beams at various load levels. These measurements are compared with predicted values for constant and varying moment regions.

Details of the four box beams tested by Stewart (1997) are shown in Table 5. All box beams have a 300 mm × 300 mm square hollow section with a 60 mm thick wall all around. Both simply supported beams, *SSB1* and *SSB2* having a clear span of 5.3 m were subjected to two equal point loads, each 1 metre away from the mid span. Continuous beams *CB1* and *CB3* have two equal clear spans of 5.9 m long, each loaded with two equal point loads, 2 m and 4 m away from the central support. All beams were reinforced with 20 mm diameter deformed bars as detailed in Table 5. Values of the slip length, l_o and the steel stress increment, Δf_{So} calculated using Eqs. (14) to (16) are also shown in the same Table.

For this comparison, primary cracks are selected from the above four beams as follows:

Constant moment regions - all the cracks developed within the constant moment region before the formation of any crack on the adjoining varying moment regions;
Varying moment regions - all cracks developed, except those formed in between existing cracks.

Measured primary crack spacings in constant moment and varying moment regions are separately arranged in ascending order and plotted as bar graphs, for comparison. These graphs shown in Fig. 11 for beams *SSB1*, *SSB2*, *CB1* and *CB3* reveal the following.

(a) Constant moment region

It can be seen in Fig. 11(a) that the measured primary crack spacings in constant moment regions of beams *SSB1* and *SSB2* vary between a minimum and a maximum value. These two limits are close to l_o and $2l_o$ as predicted by Eq. (18). Comparison of the stirrup spacings and crack spacings of these two beams clearly indicates that there is no relationship between them. Note that the distributions of primary crack spacings in these two beams are nearly identical while the stirrup spacings are entirely different (300 mm and 125 mm).

Table 5 Details of beams tested by Stewart (1997)

Beam No.	d (mm)	Deformed bars used	ρ	stirrup spacing (mm)	f_c' (MPa)	l_o (mm)	Δf_{so} (MPa)
SSB1	270	3 × 20 mm	0.0116	300	32.0	152	60
SSB2	270	6 × 20 mm	0.0232	125	27.6	126	28
CB1	266	3 × 20 mm	0.0118	125	28.9	151	56
CB3	264	6 × 20 mm	0.0228	125	26.0	125	27

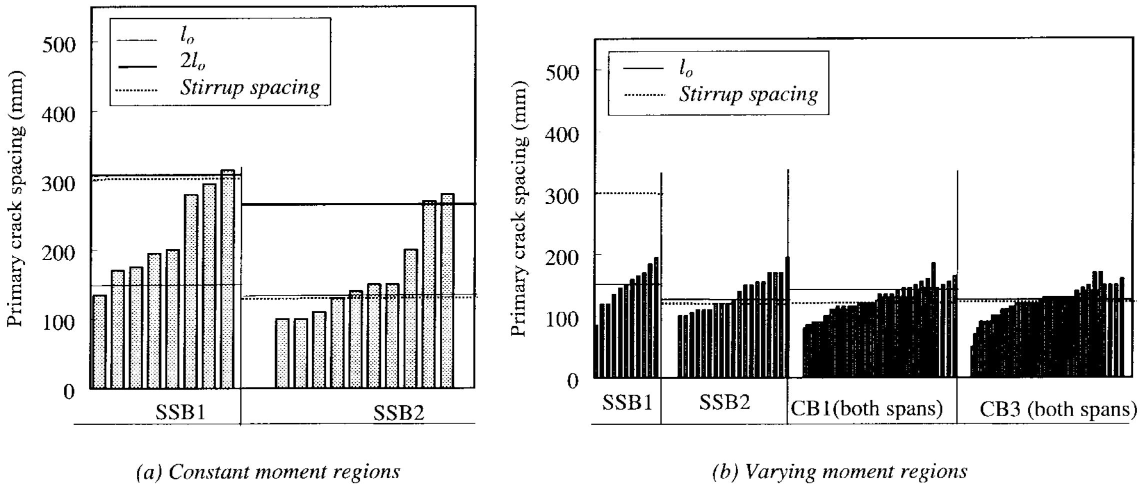

Fig. 11 Comparison of predicted primary crack spacing with those measured by Stewart (1997)

(b) Varying moment region

It can be seen in Fig. 11(b) that the measured primary crack spacings in varying moment regions of beams *SSB1*, *SSB2*, *CB1* and *CB3* vary above and below a mean value. This mean spacing is close to the calculated value of l_o, as predicted by Eq. (19). Comparison of the stirrup spacing and crack spacings in beam *SSB1* clearly shows that there is no relationship between them. Coincidentally the stirrup spacing and the slip length l_o are nearly the same in beams *SSB2*, *CB1* and *CB3*. Therefore, it is not clear whether the regular crack spacings in these three beams are related to the stirrup spacing or to the slip length l_o. However, considering the large difference between the stirrup spacing and the crack spacings in beam *SSB1*, it can be concluded that the regular crack spacings in beams *SSB2, CB1* and *CB3* are in fact related to l_o.

5.2 Average crack spacing at higher load levels (secondary cracks)

(a) Constant moment region

The average crack spacing at higher load levels in a constant moment region may vary between $0.5l_c$ and l_c, where l_c is the critical crack spacing for the particular load level (Eq. 20). The predicted average crack spacing is taken as the arithmetic mean of these two limits as $0.75l_c$ (Eq. 21). To verify this prediction, l_c values are determined using the finite element analytical procedure described in Section 2 and compared with the average crack spacing measured by Clark (1956) and Chi and Kirstein (1958) on 70 flexural members. All these beams were reinforced with deformed steel bars, with the diameter ranging from 10 mm to 35 mm. For each member, l_c is evaluated at seven steel stress levels namely, 103, 138, 172, 207, 241, 276 and 310 MPa, for which the measurements are available. This comparison is shown in Fig. 12. In this figure, the x-axis represents the calculated values of $l_{ave\text{-}pred} = 0.75l_c$ (Eq. 21) while the y-axis represents the measured values of average crack spacings. Lines corresponding to $y = l_c$ and $y = 0.5l_c$ are also shown for comparison. It is clear that most of the measured average crack spacings lie between the two limits l_c and $0.5l_c$, as predicted (Eq. 20).

The analytical procedure described in this paper for the determination of critical crack spacing l_c

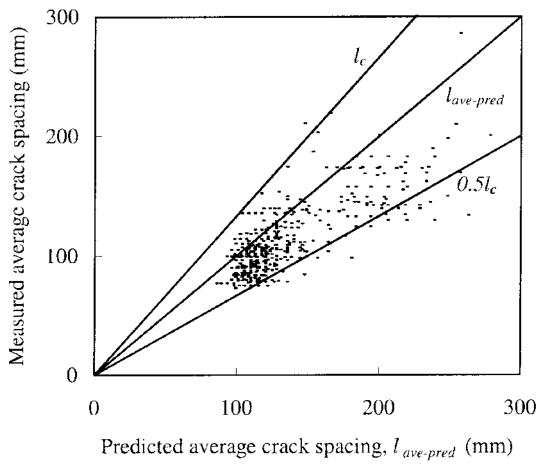

Fig. 12 Comparison of predicted average crack spacing in constant moment regions with those measured by Clark (1956) and Chi and Kirstein (1958)

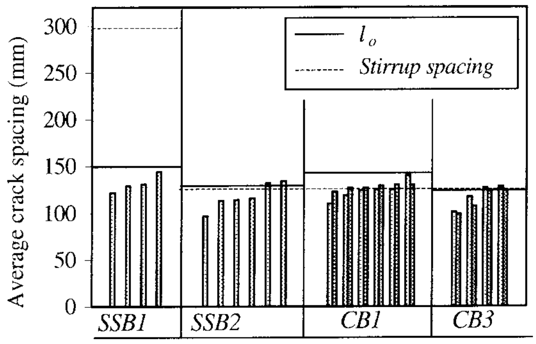

Fig. 13 Comparison of predicted average crack spacing in varying moment regions with those measured by Stewart (1997)

and maximum crack width W_t may not be suitable for practical usage, as it requires many steps of computations, including the finite element analysis. The intention of this paper is to describe the above analytical procedure, and to verify its accuracy by comparing the computed and measured spacing and width of cracks (Section 5). Empirical formulas suitable for practical usage are currently being developed, based on a large number of l_c and W_t values calculated using the procedure described herein, and will be published in a subsequent publication.

(b) Varying moment region

The average crack spacing in a varying moment region is predicted as l_o at all load levels (Eq. 22). To verify this prediction, the measured average crack spacings in varying moment regions of four box-beams *SSB1*, *SSB2*, *CB1* and *CB3* (see Table 5) tested by Stewart (1997) are compared with the calculated values of l_o in Fig. 13. In this figure, measured average crack spacings at various load levels are arranged in ascending order for each beam, and plotted as bar graphs. It can be seen that the average crack spacing at all load levels remains nearly the same, and this constant spacing is close to the calculated value of l_o, as predicted.

5.3 Maximum crack width

The maximum crack width is calculated for the same 70 flexural members tested by Clark (1956) and Chi and Kirstein (1958), already mentioned in Section 5.2(*a*). The maximum crack width at reinforcement level W_s is evaluated using the procedure described in Section 2.4 at seven steel stress levels for which the measurements are available. The corresponding crack width at the tension face is then calculated using Eq. (17). These calculated crack widths are compared with the measured values in Fig. 14(a). A similar comparison based on the Gergely and Lutz (1968) prediction procedure (Eq. 1) is shown in the accompanying Fig. 14(b). Inspection of these two figures, each containing 420 data points, indicates that the present method can calculate the maximum crack

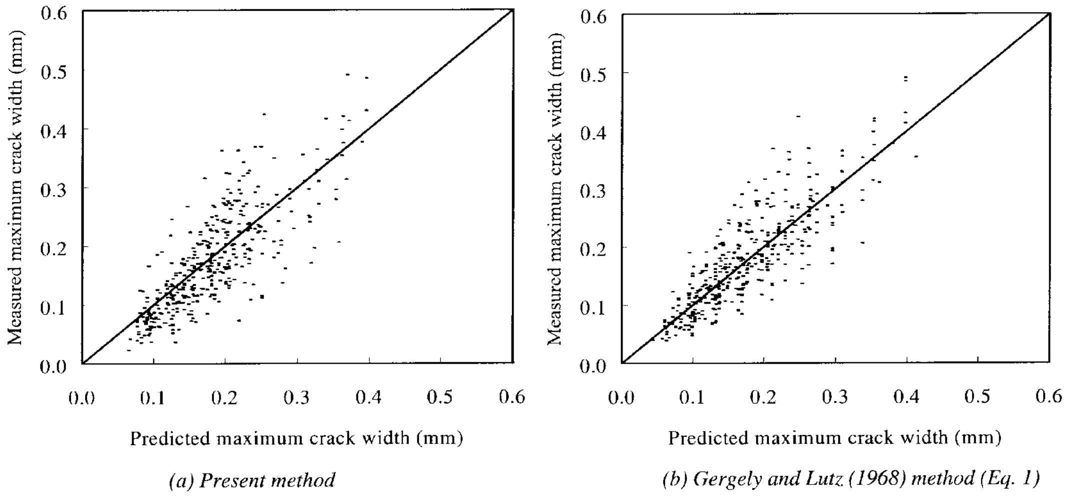

Fig. 14 Comparison of predicted maximum crack width with those measured by Clark (1956) and Chi and Kirstein (1958)

width with sufficient accuracy.

Although the present analytical method of calculating the crack width is not as simple as the use of Eq. (1), the new method has wider applicability, as it can incorporate most of the variables involved in flexural cracking. One direct application of the new method would be the investigation of the effects of different parameters on the crack width in reinforced concrete beams. This work is currently in progress and the results will be published in a subsequent publication.

6. Conclusions

Spacing and width of cracks are determined using concrete tensile stresses and displacements near flexural cracks in reinforced concrete beams. For the calculation of stresses and displacements, a free body of concrete block bounded by top and bottom faces and two transverse sections is isolated and analysed by the finite element method. The bond force acting on this free body is evaluated by using a bond stress-bond slip relationship available in literature.

Based on the stress distributions calculated by the above method, the following predictions are made with regard to the crack spacing.

(a) *in constant moment regions*: primary crack spacing varies between l_o and $2l_o$ while the average crack spacing at higher load levels lies between $0.5l_c$ and l_c.

(b) *in varying moment regions*: primary crack spacing and average crack spacing at all load levels remain constant at l_o.

In (a) and (b) above, l_o is the development length required to resist the steel stress increment that occurs at a primary crack, while l_c is the crack spacing that produces a concrete tensile stress equal to the flexural strength of concrete. The value of l_o is calculated using an empirical formula developed in this paper, while l_c is evaluated based on the results of finite element analysis. The above predictions are verified by comparing the predicted crack spacings with those measured by other investigators.

The crack width is determined as the relative difference in extensions of steel bars and surrounding concrete calculated at the crack. A comparison of the crack width values calculated by this method and those measured by other investigators reveals that they are in good agreement.

References

ACI Committee 224 (1972), "Control of cracking in concrete structures", *Proc. J.*, ACI, **69**(12).

ACI Committee 318 (1995), *Building Code Requirements for Reinforced Concrete (ACI 318-95)*, American Concrete Institute, Detriot.

Bazant, Z.P. and Oh, B.H. (1983), "Spacing of cracks in reinforced concrete", *J. Struct. Eng.*, American Society of Civil Engineers, **109**(9), 2066-2085.

Beeby, A.W. (1970), "An investigation of cracking in slabs spanning one way", *Cement and Concrete Association*, Technical Report 42.433, London.

Beeby, A.W. (1971), "An investigation of cracking on the side faces of beams", *Cement and Concrete Association*, Technical Report 42.466, London.

Broms, B.B. (1965), "Stress distribution in reinforced concrete members with tension cracks", *ACI J., Proceedings*, **62**(9), 1095-1108.

Chi, M. and Kirstein, A.F. (1958), "Flexural cracks in reinforced concrete beams", *Proc. J.*, ACI, **54**(10), 865-878.

Clark, A.P. (1956), "Cracking in reinforced concrete flexural members", *Proc. J.*, ACI, **52**(8), 851-862.

Cook, R.D., Malkus, D.S. and Plesha, M.E. (1989), *Concepts and Applications of Finite Element Analysis, Third Edition*, J. Willey.

Eligehausen, R., Bertero, V.V. and Popov, E.P. (1983), "Local bond stress-slip relationships of deformed bars under generalized excitations; Tests and analytical model", *Report No. UCB/EERC-83*, Earthquake Engineering Research Center, University of California, Berkeley, California.

Gergely, P. and Lutz, L.A. (1968), "Maximum crack width in reinforced concrete flexural members", *Causes, Mechanism, and Control of Cracking in Concrete*, SP-20, American Concrete Institute, 87-117.

Giuriani, E., Plizzari, G. and Schumm, C. (1991), "Role of stirrups and residual tensile strength of cracked concrete on bond", *J. Struct. Eng*., ASCE, **117**(1), 1-18.

Jiang, D.H., Shah, S.P. and Andonian, A.T. (1984), "Study of the transfer of tensile forces by bond", *Proc. J.*, ACI, **81**(3), 251-259.

Mains, R.M. (1951), "Measurement of the distribution of tensile and bond stresses along reinforcing bars", *Proc. J.*, ACI, **48**(3), 225-252.

Nilson, A.H. (1972), "Internal measurement of bond slip", *Proc. J.*, ACI, **69**(7), 439-441.

Standards Australia International (2001), *Concrete Structures (AS3600-2001)*, Sydney, Australia.

STRAND6 (1993), *Finite Element Analysis System*, G+D Computing Pty Ltd, New South Wales, Australia.

Stewart, R.A. (1997), "Crack widths and cracking characteristics of simply supported and continuous reinforced concrete box beams", *B. Eng Thesis*, School of Engineering, Griffith University, Gold Coast, Australia.

Venkateswarlu, B. and Gesund, H. (1972), "Cracking and bond slip in concrete beams", *J. Struct. Div., Proceedings*, American Society of Civil Engineers, **98**(ST11), 2663-2885.

Watstein, D. and Parsons, D.E. (1943), "Width and spacing of tensile cracks in axially reinforced concrete cylinders", *Journal of Research*, National Bureau of Standards, **31**(RP1545), 1-24.

Zienkiewicz, O.C. (1977), *The Finite Element Method, Third Edition*, McGraw-Hill.